Resource Allocation in SCMA-Empowered Multi-UAV Transmission System

Saumya Chaturvedi, Zilong Liu, Vivek Ashok Bohara, Anand Srivastava, Pei Xiao

***Abstract*—This research work examines the utilization of sparse code multiple access (SCMA) in improving downlink communication for multiple unmanned aerial vehicles (UAVs) network, whereby SCMA is a disruptive multiple access technique for future massive machine-type communications (mMTC). The goal is to maximize the sum-rate of the ground users by optimizing the UAV three-dimensional deployment location, user-UAV association, SCMA subchannels, power and bandwidth allocation. Due to the complex and non-convex nature of the formulated optimization problem, obtaining the global optimal solution is infeasible. To address this problem, we propose to decompose the overall problem into four manageable subproblems and solve them sequentially. The user clustering and UAV deployment problem are tackled using a modified K-means algorithm, while the three proposed methods leveraging the channel state information and frequency reuse address the subchannel assignment subproblem. Further, iterative heuristic algorithms are then developed to optimize power and bandwidth allocation, thereby improving both sum-rate and the outage performance. The simulation results demonstrate significant performance improvements with the proposed methodologies, highlighting the potential of SCMA-assisted UAV networks over traditional orthogonal multiple access techniques.**

***Index Terms*—Probabilistic line-of-sight channel model, resource allocation, sparse code multiple access (SCMA) technique, sum-rate, unmanned aerial vehicles (UAV) communications.**

I. Introduction

The widespread integration of fifth-generation (5G) communication systems has motivated global researchers toward the development of sixth-generation (6G) wireless systems, engaging both academia and industries [1]. In the realm of 6G, the objective is to enhance data services to progressively meet the stringent quality-of-service (QoS) requirements, encompassing aspects such as data rate, reliability, latency, connection density, spectrum efficiency, energy efficiency, and more. In particular, 6G will continue to deal with an explosive growth of the Internet of Things (IoT) devices. The number of mobile users and Internet-enabled devices is projected to exceed 40 billion in the coming years [2]. Such an overwhelming demand for massive connectivity drastically calls for high spectrally efficient multiple access schemes [3].

In recent times, unmanned aerial vehicles (UAVs) have been utilized in various applications, including but not limited to goods delivery, rapid rescue operations, traffic surveillance, etc. [4]. Among numerous applications, the usage of UAVs in communications is particularly compelling. Thanks to their agility and maneuverability, UAVs can improve the likelihood of establishing line-of-sight (LoS) connectivity with the ground users (GUs) [5]. In challenging geographical conditions, UAVs can be used as aerial base stations (BSs) or relays to facilitate recovery of communication.

Conventional orthogonal multiple access (OMA) schemes face limitations in supporting efficient communication between UAVs and mMTC devices on the ground. In contrast, non-orthogonal multiple access (NOMA) techniques have been a focal point of extensive research due to their ability to support a greater number of simultaneously serviced devices, reducing latency, while achieving higher data rate [3].

The fundamental concept of NOMA is to accommodate a large number of devices by non-orthogonally overloading resource elements (REs). NOMA is mainly classified into code-domain NOMA (CD-NOMA) and power-domain NOMA (PD-NOMA). PD-NOMA involves assigning varied power levels to multiple GUs depending on their channel conditions and spatial locations [6]. In CD-NOMA, on the other hand, each of the user is allocated a unique codebook (CB) or signature sequence. In this paper, we are interested in sparse code multiple access (SCMA) which is one of the prominent CD-NOMA schemes. SCMA is a technique that utilizes multidimensional CBs to enhance multiuser capacity and connectivity [7]. In SCMA, each user directly maps its input bits to a codeword drawn from its associated CB. This approach extends the aspects of code division multiple access (CDMA) to multi-dimensional domain [8]. In field trials, SCMA has demonstrated significant performance enhancements, offering up to three times the system throughput while maintaining link performance as of OMA [9]. The SCMA system differs from other communication system. At the receiver, the CB sparsity can be fully exploited by utilizing message passing algorithm (MPA) to perform decoding with low complexity. The coding gain and constellation shaping gain in SCMA leads to outstanding bit error rate (BER) and sum-rate performances [10], [11]. Moreover, various low-complexity decoding schemes have been proposed in literature for static [12] and mobile scenario [13]. Building on these advancements, this work examines SCMA's role

Saumya Chaturvedi, Vivek Ashok Bohara, and Anand Srivastava are with Indraprastha Institute of Information Technology Delhi (IIIT-Delhi), 110020, India (e-mail: {saumyac, vivek.b, anand}@iiitd.ac.in). Zilong Liu is with the School of Computer Science and Electronics Engineering, University of Essex, U.K. (e-mail: zilong.liu@essex.ac.uk). Pei Xiao is with Institute of Communication Systems (ICS), 5GIC & 6GIC, University of Surrey, UK (e-mail: p.xiao@surrey.ac.uk).

The work of Z. Liu was supported in part by the UK Engineering and Physical Sciences Research Council under Grants EP/X035352/1 ("DRIVE") and EP/Y000986/1 ("SORT"), and by the British Council under Grant UKIERI-SPARC/01/22.

in a multi-UAV network, focusing on efficient resource management to evaluate its performance benefits.

A. Related Works

The recent development of the integration of NOMA with UAV has led to several works in the literature, as discussed in Table I. For example, the paper [14] presented a large-scale multi-UAV NOMA framework using stochastic geometry, addressing UAV-centric offloading and user-centric emergency services under imperfect successive interference cancellation (SIC) conditions. The paper [15] worked on optimizing UAV precoding in uplink NOMA cellular-connected UAV networks to maximize sum-rate and mitigate interference using SIC. The authors in [16] worked on a cellular-connected aerial user equipment (AUE) periodically transmitting to a BS for surveillance or monitoring applications. Here, PD-NOMA was utilized for simultaneous transmission from the AUE and GU for an efficient spectrum usage, while AUE moving along a given trajectory.

In [17], an uplink relay based multi-UAV system was presented, for IoT applications in disaster scenario. The study in [18] analysed the capacity of full-duplex (FD) NOMA-UAV networks through a moment generating function (MGF) approach. Dang *et al.* [19] studied the throughput of a NOMA-aided cognitive radio (CR) system with multiple UAVs as relays. The paper [20] proposed secure transmission schemes for UAV-NOMA networks, optimizing UAV placement, power allocation, and beamforming to protect users against eavesdropping under single and multiple secure user scenarios. The authors in [21] worked on multi-UAV uplink network in which authorized UAVs executed NOMA transmission amidst the existence of eavesdropping UAVs.

It is noted that NOMA becomes helpful in utilizing the UAVs features, even for single antenna GUs. In NOMA-assisted multi-UAV networks, researchers have worked on different optimization variables such as user clustering and association [22]–[24], scheduling [25], UAVs placement [22], [26]–[28], power allocation [22]–[25], [27], [28], UAVs trajectories [23] and subchannel assignment [27]. Various performance objectives have been improved, including capacity [17], [22], [27]–[30], energy efficiency (EE) [25], [31]–[33], uplink energy minimization [23] and delay [34].

The work in [23] studied the joint optimization of user pairing, UAV trajectories, association between user and UAV, and power allocation for NOMA-aided multi-UAV uplink networks. The study in [25] focused on a NOMA-enabled multi-UAV-assisted IoT system, optimizing scheduling, power allocation, and UAV trajectories to improve throughput and EE. The study in [26] proposed a multi-UAV coverage scheme aimed at maximizing the average UAV capacity while ensuring full GU coverage. In [28], the three-dimensional (3D) deployment of UAV and user power allocation were optimized to maximize the sum rate. In [27], the system capacity was maximized in a NOMA multi-UAV IoT uplink framework through joint optimization of subchannel assignment, transmit power for IoT sensors, and UAV altitudes. In [24], a multi-UAV-assisted IoT sensor system with NOMA was optimized to maximize the total utility of IoT sensor bit rates.

In [31], the EE was maximized in a NOMA-enabled UAV network, where multiple UAVs equipped with multiple antennas concurrently served towards energy receivers (ERs) and information receivers (IRs). In [32], the study investigated the optimization of 3D deployment of multiple UAVs, resource allocation, and association of UAV users within a NOMA-assisted mobile edge computing (MEC) uplink network. Similarly, [33] examined the EE of a UAV-enabled NOMA-MEC framework, where multiple UAVs functioned as edge servers to support computational tasks for GUs.

In [35], the authors proposed a cooperative NOMA scheme to mitigate severe interference for a cellular-UAV integrated uplink network. The authors in [36] and [37] also worked on cooperative multi-UAV NOMA frameworks, where the former optimized the distribution of multi-user detection tasks among UAVs to maximize sum-rate, while the latter employed index modulation to avoid error-prone SIC decoding. In [38], NOMA-enabled multi-UAV caching framework was proposed to minimize the content retrieval delay using deep reinforcement learning (DRL) approach. A comprehensive overview of RL techniques for enhancing autonomy and optimizing decision-making in multi-UAV networks, with applications in resource allocation, trajectory planning, and network management is presented in the survey paper [39].

The authors in [40] introduced the aerial intelligent reflecting surface (AIRS)-assisted mmWave networks, which involved equipping each BS with an AIRS swarm to enhance the area spectral efficiency (ASE) and coverage in the downlink communications. In [41], RSMA-based multicast communication was studied for a satellite and aerial-integrated network (SAIN) to enhance sum rate for content delivery scenario. The authors in [42] and [43] worked on improving the system secrecy EE (SEE) in a multibeam satellite systems.

B. Motivations and Contributions

The literature review above indicates that NOMA-aided UAV systems can provide enhanced QoS. However, the existing works predominantly concentrate on the PD-NOMA scheme. The efficacy of PD-NOMA in supporting UAV communications can not be assured because of several factors. Firstly, the reliance on a flawless decoding technique at the receiver, such as successive interference cancellation (SIC), raises concerns as its feasibility may need to be guaranteed in complex wireless channels. Secondly, PD-NOMA relies on a near-far user pairing strategy, where one user experiences a strong channel while the other has a weaker channel. With appropriate power allocation, this approach enables PD-NOMA to achieve performance gains over OMA. However, the pairing process introduces significant complexity, particularly in dynamic environments. In contrast, SCMA does not require near-far user pairing to achieve superior performance compared to OMA. SCMA enables multiple users to efficiently share a resource block, eliminating the

TABLE I
COMPARISON OF THE PROPOSED WORK WITH PRIOR UAV-NOMA STUDIES

Reference	UAV Position	User-UAV Association	Subchannel Allocation	Power Allocation	Bandwidth Allocation	Objective
[16]	UAV Height and Trajectory	✗	✗	✗	✗	Analyzed the rate coverage probability in a cellular AUE network.
[17]	✓	✗	✗	✓	✗	Maximized uplink capacity in a UAV-based IoT network using NOMA, with UAVs collecting data and relaying to the terrestrial BS.
[22]	✓	✗	✗	✓	✗	Maximize throughput for UAVs-assisted FD NOMA system based cellular network.
[23]	UAV trajectories	✓	✗	✓	✗	Minimize energy consumption while ensuring successful data transmission to UAV-BSs.
[24]	✓	✓	✗	✓	✗	Maximize the sum utility of bit rates of all IoT sensors.
[25]	UAV trajectory	✗	✗	✓	✗	Proposed a NOMA-enabled multi-UAV-enabled IoT system to enhance user capacity and UAV EE.
[26]	✓	✗	✗	✗	✗	Developed multi-UAV coverage scheme to maximize capacity while ensuring coverage for all GUs.
[27]	✓	✗	✓	✓	✗	Maximized capacity of multi-UAV enabled IoT NOMA uplink transmission system for LoS channel.
[28]	✓	✗	✗	✓	✗	Maximized network sum-rate with UAVs using OMA across and NOMA within sub-clusters.
[30]	✓	✗	✗	✗	✗	Maximized the sum log-rate utility for NOMA-UAV BSs.
[31]	✓	✗	✗	✓	✗	Maximized EE in single and multi UAV-NOMA network to serve both IRs and ERs in downlink and uplink.
[32]	✓	✓	✗	✓	✗	Maximized EE in a NOMA-assisted MEC uplink network.
[33]	UAV trajectory	✗	✗	✓	✗	Worked on multi-UAV-assisted NOMA integrated MEC network for task offloading.
[34]	✗	✗	✗	✓	✗	Formulated a min-max delay optimization problem for NOMA-enabled multiple UAV emergency networks.
[35]	✗	✗	✗	✓	✗	Maximized weighted sum-rate using NOMA for uplink cooperative NOMA for cellular-connected UAV under strong LoS A2G channels.
[40]	✗	✓	✗	✗	✗	Evaluated the ASE and coverage probability of large-scale AIRS-assisted mmWave networks.
[44]	✗	✗	✓	✓	✗	Maximize the downlink rate in a multi-UAV multi carrier (MC)-NOMA network with relay UAVs and distance-dependent path loss.
Proposed work	✓	✓	✓	✓	✓	Maximization of sum-rate for a SCMA based multi-UAV network under probabilistic path-loss channel model.

need for complex pairing mechanisms and overcoming a key challenge of PD-NOMA.

To the best of our understanding, limited research has been undertaken to explore the potential performance enhancements in UAV networks networks facilitated by SCMA [45]–[48]. SCMA presents a promising alternative due to its enhanced robustness and flexibility in diverse and dynamically changing environments [49]. Additionally, it reduces the dependency on precise power control, which is a critical requirement in traditional PD-NOMA systems.While SCMA renders the connectivity problem, high interference necessitates the sophisticated management of resources to obtain desired QoSs. This work investigates the potential of SCMA in UAV-assisted communication networks by addressing several key challenges. First, UAV deployment optimization plays a critical role in enhancing SCMA performance. It requires balancing signal strength with inter- and intra-UAV interference. To optimize this, a modified K-means algorithm is employed for 2D UAV positioning, helping to improve SCMA performance and reduce interference. Second, interference management is particularly challenging due to SCMA's resource block structure, where subchannels are assigned to serve multiple users, and each user utilizes multiple subchannels for communication. This user-subcarrier mapping becomes even more complex in multi-UAV networks, where the interactions between UAVs and users significantly impact both inter- and intra-UAV interference.

In this context, it is crucial to carefully manage the allocation of REs by selecting the appropriate subset of REs for each UAV in order to mitigate interference. Once the subset of REs is determined, the next step involves allocating subchannels from this subset to the users associated with the UAV to minimize interference and optimize system performance. Finally, the optimal allocation of bandwidth and power for each subchannel is crucial for improving system performance, as these resources are interdependent. Thus, the development of efficient algorithms is crucial to

overcome these challenges and maximize the potential of SCMA in UAV-enabled communication systems. The primary contributions of the proposed work are:

- We investigate a multi-UAV downlink system where UAVs, supported by SCMA, function as aerial BSs to serve GUs. Unlike conventional approaches, our work jointly optimizes key system parameters, including UAV 3D deployment, user clustering, UAV-user association, subchannel assignment, power allocation, and bandwidth allocation, to maximize the sum rate.
- To handle the complexity of the formulated mixed-integer nonconvex optimization problem, we propose a novel decomposition strategy, dividing it into four interrelated subproblems. Unlike existing works that address these aspects separately, our framework ensures coordinated optimization across multiple dimensions:
  - For UAV 2D deployment, we use a modified K-means algorithm to ensure equitable user allocation and balanced resource utilization. For UAV altitude optimization, we apply golden section search (GSS) to optimize the UAV heights.
  - We introduce three frequency reuse-based subchannel assignment schemes designed to mitigate both intra-UAV and inter-UAV interference, improving spectral efficiency.
  - We propose iterative algorithms for power and bandwidth allocation, specifically designed to enhance outage performance while maintaining efficient resource distribution.
- The simulation results show that the proposed resource allocation schemes enhance multi-UAV SCMA performance, outperforming the benchmark schemes in terms of sum rate and outage performance.

The paper is organized as follows: Section II presents the multi-UAV SCMA system model and discuss the formulated optimization problem. Section III presents the proposed solution to the optimization problem. Section IV presents and analyzes the simulation results. Section V provides the conclusion. In this paper, scalars, vectors, and matrices are denoted by regular, bold lowercase, and bold uppercase letters, respectively. The set of real, binary, and complex numbers are denoted by $\mathbb{R}$, $\mathbb{B}$ and $\mathbb{C}$, respectively. The natural logarithm of x is denoted as $\log(x)$, and the absolute value of a complex number x is represented by $|x|$.

II. System Model and Optimization Problem Formulation

A. System Model

As shown in Fig. 1, an SCMA-aided downlink network is considered, with multiple hovering UAVs working as aerial-BSs, serving a total of M single-antenna users over K_{net} REs. Let the set of UAVs, users and total network REs be denoted as $\mathcal{N} = \{1, 2, \cdots, N\}, \mathcal{M} = \{1, 2, \cdots, M\}$ and $\mathcal{K}_{\text{net}} = \{1, 2, \cdots, K_{\text{net}}\}$, respectively. The assumption is made that the users are stationary, and their locations are known by a control center. Let the locations of user

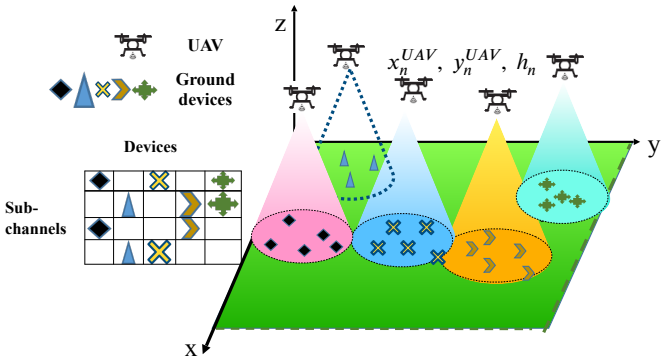

Fig. 1. Multi-UAV SCMA system model with ground devices communicating over multiple sub-channels. For the sake of clarity, only five devices subchannel allocation are shown.

$m \in \mathcal{M}$ and UAV $n \in \mathcal{N}$ be denoted by $\mathbf{x}_m = (x_m, y_m)$ and $\mathbf{l}_n = (x_n^{\text{uav}}, y_n^{\text{uav}}, h_n^{\text{uav}})$, respectively.

Due to the limited UAV coverage, we assume that each UAV can serve (M/N) devices. If M is not a multiple of N, each UAV serves either $\lfloor M/N \rfloor$ or $\lceil M/N \rceil$ devices. It is assumed that, K orthogonal subchannels are allocated to each UAV-BS, where $K < K_{\text{net}}$. Let J_n represent the number of users served by the nth UAV, such that $M = \sum_{n=1}^{N} J_n$ and the corresponding set is denoted as $\mathcal{J}_n$ such that $\mathcal{J}_{n1} \cap \mathcal{J}_{n2} = \emptyset, \forall n_1, n_2 \in \mathcal{N}, n_1 \neq n_2$.

1) A2G Channel Model: Thanks to UAV's agile moving nature, it is assumed that LoS connections can be kept for most devices. Nevertheless, potential disruptions in UAV-to-ground device connections may arise due to blockages, particularly in urban areas. Consequently, we are exploring a probabilistic LoS channel model that incorporates both the LoS and non-LoS (NLoS) components, contingent upon the specific environment in which the UAV is deployed [4]. The LoS probability between the mth user and the nth UAV-BS is expressed as [50]:

$$\mathbb{P}_m^L[n] = \frac{1}{1 + ae^{-b(\theta_m^n - a)}}, \tag{1}$$

where, the constants a and b are dependent on the environmental conditions [51]. The symbol θ_m^n represents the elevation angle, measured in degrees, indicating the angle from the mth user to the nth UAV-BS. It is given as $\theta_m^n = (\frac{180}{\pi})\tan^{-1}(\frac{h_n^{\text{uav}}}{r_m^n})$, where r_m^n indicates the 2D distance from the nth UAV-BS to the mth user. In a corresponding manner, NLoS probability is $\mathbb{P}_m^{NL}[n] = 1 - \mathbb{P}_m^L[n]$. Further, the path loss for the LoS and NLoS components are: [50]

$$\text{PL}_m^{\text{LoS}}[n] = \left(\frac{4\pi f_c d_m^n}{c}\right)^{\alpha} \eta_{\text{LoS}}, \tag{2}$$

$$\text{PL}_m^{\text{NLoS}}[n] = \left(\frac{4\pi f_c d_m^n}{c}\right)^{\alpha} \eta_{\text{NLoS}}, \tag{3}$$

where α represents the path loss exponent, d_m^n represents the 3D distance from the nth UAV-BS to the mth user and c is the speed of light. The path loss coefficients for the LoS and

TABLE II
KEY MATHEMATICAL NOTATIONS AND DESCRIPTIONS

Notation	Description
M	Total network users
N	Total network UAVs
$\mathcal{K}_{\text{net}}$	Total network subchannels
$\mathbf{x}_m$	2D location of the mth user
$\mathbf{l}_n$	3D location of the nth UAV
J_n	Count of users served by UAV n
K	Count of subchannels allocated to each UAV-BS
θ_m^n	Elevation angle from mth user to UAV-BS n
r_m^n	2D distance between UAV-BS n and mth user
$\mathbb{P}_m^L[n]$	LoS link probability between mth user and UAV-BS n
$\mathbb{P}_m^{NL}[n]$	NLoS link probability between mth user and UAV-BS n
$\text{PL}_m^{\text{LoS}}[n]$	LoS component Path loss
$\text{PL}_m^{\text{NLoS}}[n]$	NLoS component Path loss
$g_{n,k,m}$	Channel gain between UAV n and mth user on subchannel k
$f_{m,n,k}$	Subchannel assignment of the kth subchannel to user m by nth UAV
$p_{n,k,j}$	Power allocated by UAV n to user j on subchannel k
$I_{n,k,j}^{\text{intra}}$	Intra-UAV interference faced by the jth user associated with nth UAV on the kth subchannel
$I_{n,k,j}^{\text{inter}}$	Inter-UAV interference faced by the jth user associated with nth UAV on the kth subchannel
$\gamma_{n,k,j}$	SINR of jth user associated with nth UAV at the kth subchannel
$c_{n,j}$	Binary variable to indicate the association between user j and UAV n
$v_{n_i,k}$	bandwidth allocation factor of the k-th subchannel in the n_ith UAV subgroup

NLoS paths are represented by η_{LoS} and η_{NLoS}. The average path loss between the mth user and the nth UAV is:

$$\mathbb{L}_{n,m} = \mathbb{P}_m^L[n]\ \text{PL}_m^{\text{LoS}}[n] + \mathbb{P}_m^{NL}[n]\ \text{PL}_m^{\text{NLoS}}[n].$$

Considering small-scale fading, the channel gain between UAV n and mth user at subchannel k is given by:

$$g_{n,k,m} = H_{n,k,m}\ .\ 10^{-\mathbb{L}_{n,m}/10}, \tag{4}$$

where $H_{n,k,m}$ denotes the fading coefficient between UAV n and user m at the kth subchannel [52]. Table II summarizes the primary notations and their respective descriptions.

2) SCMA Data Transmission Model: In SCMA, binary data are directly mapped to complex multidimensional codewords selected from the associated CB. The codewords are sparse complex vectors characterized by a predetermined d_v non-zero values, where $K > d_v$. The enhancement of SCMA's performance compared to other NOMA schemes relies on the careful design of these sparsely structured CBs. The CB of a user is distinctly defined by its pattern of sparsity. In SCMA, the CB design requires determining the optimal mapping matrix $\mathbb{T}^*$, and multidimensional constellation $\mathbf{A}^*$, respectively. The j-th user CB with dimensions $K \times \hat{M}$ can be given by:

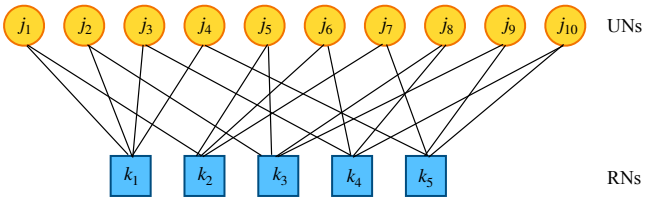

Fig. 2. An SCMA 5×10 factor graph with $d_f = 4$ and $d_v = 2$, where circle denotes the user nodes and square denotes the resource nodes.

$$\text{CB}_j = \mathbb{T}_j \Delta_j \mathbf{A}_{\text{MC}}, \quad \forall j = 1, \cdots, J, \tag{5}$$

where $\mathbb{T}_j \in \mathbb{B}^{K \times d_v}$ signifies the mapping matrix, Δ_j signifies the jth user constellation operator, and $\mathbf{A}_{\text{MC}}$ signifies the mother constellation. The mapping matrix $\mathbb{T}_j$ is chosen so that jth user is activated only on a particular set of REs. Moreover, it is crucial to take into account key performance indicators (KPIs) like Euclidean distance, kissing number (both Euclidean and Product), and diversity order when designing $\mathbf{A}_{\text{MC}}$.

SCMA is characterized by its sparse CBs, with user-RE associations represented through a bipartite factor graph (BFG). In a regular BFG, every user node (UN) connects to d_v resource nodes (RNs), and conversely, every RN is connected to d_f UNs. Fig. 2 demonstrates the RE-user association for a 5×10 SCMA block by a BFG, where each circle denote UN and square box denote RN. In this graph, the first RN is connected to the first four UNs, signifying that these users share the first RE. Alternatively, it can be represented by a factor graph matrix (FGM) $\mathbf{F}_{5\times10}$ with elements $f_{k,j}$, where $k \in \{1, \ldots, 5\}$ and $j \in \{1, \ldots, 10\}$ [7]. In a 5×10 SCMA block, ten users data is transmitted through five subchanels, resulting in an overloading factor equal to $10/5 = 2$. The jth column of the FGM is $\mathbf{f}_j = \text{diag}(\mathbb{T}_j \mathbb{T}_j^T)$. The $\mathbf{F}_{5\times10}$ FGM corresponding to the BFG depicted in Fig. 2 is given as [53]

$$\mathbf{F}_{5\times10} = \begin{bmatrix} 1 & 1 & 1 & 1 & 0 & 0 & 0 & 0 & 0 & 0 \\ 1 & 0 & 0 & 0 & 1 & 1 & 1 & 0 & 0 & 0 \\ 0 & 1 & 0 & 0 & 1 & 0 & 0 & 1 & 1 & 0 \\ 0 & 0 & 1 & 0 & 0 & 1 & 0 & 1 & 0 & 1 \\ 0 & 0 & 0 & 1 & 0 & 0 & 1 & 0 & 1 & 1 \end{bmatrix}. \tag{6}$$

Let (n, j) denote the index of the jth user associated with nth UAV. The central controller allocates K subchannels to each UAV. Thus, UAVs are assumed to share some of the spectrum, whereby each UAV employs SCMA to provide data services to the GUs. The received signal at subchannel k is affected by both inter-UAV interference and intra-UAV interference. Here, the variable $f_{m,n,k}$ indicates the association of device m with the nth UAV on the kth subchannel. If device m_1 associated with UAV n_1 shares subchannel k with device m_2 associated with UAV n_2, then $f_{m_1,n_1,k} = f_{m_2,n_2,k} = 1$, meaning that inter-UAV

interference exists between the two users. Also, if two users associated with the same UAV share the same sub-channel, then there exists intra-UAV interference between them. Let $p_{n,k,j}$ be the power allocated by the nth UAV to the jth user on kth subchannel. Hence, the received signal at the (n,j) user is:

$$y_{n,j} = \underbrace{\sum_{k=1}^{K_{net}} c_{n,j} g_{n,k,j} f_{n,k,j} x_{n,k,j}}_{\text{Desired signal}} + \underbrace{\sum_{k=1}^{K_{net}} \sum_{\substack{i \in \mathcal{J}_n \\ i \neq j}} c_{n,i} g_{n,k,i} f_{n,k,i} x_{n,k,i}}_{\text{Intra-group interference}} + \underbrace{\sum_{\substack{n' \in \mathcal{N} \\ n' \neq n}} \sum_{k=1}^{K_{net}} \sum_{i=1}^{\mathcal{J}_{n'}} c_{n',i} g_{n',k,i} f_{n',k,i} x_{n',k,i}}_{\text{Inter-group interference}} + \underbrace{w_{n,j}}_{\text{Noise}}. \quad (7)$$

Therefore, the decoding signal-to-interference-plus-noise ratio (SINR) for user (n,j) at subchannel k is:

$$\gamma_{n,k,j} = \frac{g_{n,k,j} p_{n,k,j}}{I^{\text{intra}}_{n,k,j} + I^{\text{inter}}_{n,k,j} + v_{n_i,k}\sigma^2}, \quad (8)$$

where

$$I^{\text{intra}}_{n,k,j} = \sum_{\substack{i \in \mathcal{J}_n \\ i \neq j}} c_{n,i} ||g_{n,k,i}||^2 f_{n,k,i}\ p_{n,k,i},$$

$$I^{\text{inter}}_{n,k,j} = \sum_{\substack{n' \in \mathcal{N} \\ n' \neq n}} \sum_{i=1}^{J_{n'}} c_{n',i} ||g_{n',k,i}||^2 f_{n',k,i}\ p_{n',k,i}$$

where σ^2 represents the variance of additive white Gaussian noise (AWGN). Here, we present a binary variable $c_{n,j}$ to indicate the association between user j and UAV n. The variable $c_{n,j}$ is set to 1 if $\sum_{k=1}^{K} f_{n,k,j} \geq 1$, indicating user j is associated with UAV-BS n; otherwise, $c_{n,j} = 0$. The bandwidth allocation factor for subchannel k in the n_ith UAV subgroup is denoted as $v_{n_i,k}$. Thus, the data rate of user (n,j) is $\mathbf{R}_{n,j} = \sum_{k=1}^{K} v_{n_i,k} \log_2(\gamma_{n,k,j})$.

B. Problem Formulation

We aim to maximize the sum rate by jointly optimizing the UAV 3D deployment $\mathbf{L} = \{\mathbf{l}_n, \forall n \in \mathcal{N}\}$, user associations $\mathbf{C} = \{c_{n,j}, \forall n \in \mathcal{N}, j \in \mathcal{J}\}$, subchannel assignments $\mathbf{F} = \{f_{n,k,j}, \forall n \in \mathcal{N}, k \in \mathcal{K}, j \in \mathcal{J}_n\}$, power allocation $\mathbf{P} = \{p_{n,k,j}, \forall n \in \mathcal{N}, k \in \mathcal{K}, j \in \mathcal{J}_n\}$ and bandwidth allocations $\mathbf{V} = \{v_{n_i,k}, \forall n_i \in \mathcal{N}_i, k \in \mathcal{K}_{\text{net}}\}$. Let $\mathbf{G} = \{g_{n,k,m}, \forall n \in \mathcal{N}, k \in \mathcal{K}, m \in \mathcal{M}\}$ denotes the channel gain matrix, and $\mathbf{S} = \{\gamma_{n,k,j}, \forall n \in \mathcal{N}, k \in \mathcal{K}, j \in \mathcal{J}_n\}$ denotes the SINR matrix. The joint optimization problem is mathematically expressed as follows:

$$\mathcal{P}(1): \max_{\mathbf{L},\mathbf{C},\mathbf{F},\mathbf{P},\mathbf{V}} \quad \sum_{n=1}^{N} \sum_{j=1}^{J_n} \mathbf{R}_{n,j} \quad (9a)$$

$$\text{s.t. } 0 \leq x^{\text{uav}}_n, y^{\text{uav}}_n \leq l_{\max}, H_{\min} \leq h^{\text{uav}}_n \leq H_{\max}, \ \forall n \in \mathcal{N}, \quad (9b)$$

$$c_{n,m} \in \{0,1\}, \ \forall\ n \in \mathcal{N}, m \in \mathcal{M}, \quad (9c)$$

$$\left\lfloor \frac{M}{N} \right\rfloor \leq \sum_{m=1}^{J_n} c_{n,m} \leq \left\lceil \frac{M}{N} \right\rceil, \forall n \in \mathcal{N} \quad (9d)$$

$$\sum_{n=1}^{N} c_{n,m} = 1, \forall m \in \mathcal{M} \quad (9e)$$

$$f_{n,k,j} \in \{0,1\}, \ \forall\ n \in \mathcal{N}, k \in \mathcal{K}, j \in \mathcal{J}_n, \quad (9f)$$

$$\sum_{k=1}^{K_{\text{net}}} \text{nnz}(\mathbf{F}(n,k,:) = K, \ \forall\ n \in \mathcal{N}, \quad (9g)$$

$$\mathbf{F}_{n,j} \neq \mathbf{F}_{n,j'}, \quad \forall\ n \in \mathcal{N}, j \neq j' \in \mathcal{J}_n, \quad (9h)$$

$$\sum_{j=1}^{J_n} f_{n,k,j} \leq d_f, \quad \forall\ n \in \mathcal{N}, k \in \mathcal{K}, \quad (9i)$$

$$\sum_{k=1}^{K} f_{n,k,j} \leq d_v, \quad \forall\ n \in \mathcal{N}, j \in \mathcal{J}_n, \quad (9j)$$

$$p_{n,k,j} \geq 0, \ \forall\ n \in \mathcal{N}, k \in \mathcal{K}, j \in \mathcal{J}_n, \quad (9k)$$

$$\sum_{k=1}^{K} \sum_{j=1}^{J_n} f_{n,k,j} p_{n,k,j} \leq \text{P}_{\text{tot}}, \ \forall\ n \in \mathcal{N}, \quad (9l)$$

$$\sum_{k=1}^{K_{\text{net}}} v_{n_i,k} = K_{\text{net}}, \ \forall\ n_i \in \mathcal{N}_i, \quad (9m)$$

where P_{tot} signifies the overall allocated transmit power for communication at each of the UAV-BS. Constraint (9c) indicates that the UAV-BSs 2D coordinates are inside the maximum defined length $l_{\max}$ in which the users are located and their height lie between $H_{\min}$ and $H_{\max}$. Constraints (9d) and (9g) indicate that $c_{n,m}$ and $f_{n,k,j}$ have binary values, respectively. Constraint (9e) is imposed to guarantee that each of the UAV-BS offers services to an equivalent number of GUs. Constraint (9f) specifies that each user is serviced by precisely single UAV-BS. Constraint (9h) specifies that each of the UAV-BS employs K number of subchannels. Constraint (9i) ensures that the FGM designed for each group should not have any identical columns. Constraint (9j) indicates that maximum d_f number of users can communicate over each subchannel, while constraint (9k) signifies that each user is active over d_v subchannels. Constraint (9m) specifies that power allocated to the users among all subchannels should be less or equal to P_{tot}. Constraint (9n) denotes that the sum of the bandwidth allocation factor is K_{net} for each UAV subgroup.

However, solving the optimization problem $\mathcal{P}(1)$ is challenging, as these optimization variables exhibit high coupling, and the objective function is neither concave nor convex

concerning these variables. Additionally, the association and FGM design introduces binary variables, thus bringing integer constraints into (9d)-(9k). As a result, problem $\mathcal{P}(1)$ constitutes a mixed-integer non-convex optimization problem, making the search for a globally optimal solution challenging [54].

III. Proposed Solution

To compute a suboptimal solution of $\mathcal{P}(1)$, we decompose the overall problem into four subproblems and solve them sequentially. Initially, we determine the UAV-BS–user associations and UAV-BS 3D placements. Subsequently, we execute the subchannel allocation to all the UAV-BSs of the network with a priority on minimizing interference. Further, the powers allocated to each user at each active subchannel are optimized. Finally, bandwidth allocation is done for each subchannel such that the total bandwidth allocated to each UAV subgroup is fixed. This problem transformation and solution approach is shown by Fig. 3.

A. Users clustering and UAVs deployment

For a given $\mathbf{F}$, $\mathbf{P}$ and $\mathbf{V}$, the joint UAV placement and user clustering problem becomes

$$\mathcal{P}(\text{A1}): \quad \max_{\mathbf{L},\mathbf{C}} f_{\text{A1}}(\mathbf{L},\mathbf{C}) = \sum_{n=1}^{N}\sum_{j=1}^{J_n} \mathbf{R}_{n,j} \tag{10a}$$

$$\text{s.t.} \quad (9\text{c}), (9\text{d}), (9\text{e}), (9\text{f}). \tag{10b}$$

To address problem $\mathcal{P}(\text{A1})$, we decompose it into two distinct components: (1) the identification of UAV 2D deployment locations and users clustering, (2) the determination of UAV-BSs altitude. The mathematical expression for the first component, involving users clustering and UAV 2D deployment, is as follows:

$$\mathcal{P}(\text{SP}_1): \quad \min_{x_n^{\text{uav}}, y_n^{\text{uav}}, c_{n,m}} \sum_{n=1}^{N}\sum_{m=1}^{M} c_{n,m} r_m^n \tag{11a}$$

$$\text{s.t.} \quad 0 \le x_n^{\text{uav}}, y_n^{\text{uav}} \le l_{\max}, \tag{11b}$$

$$(9\text{d}), (9\text{e}), (9\text{f}). \tag{11c}$$

In the subproblem $\mathcal{P}(\text{SP}_1)$, the cost function is defined as the summation of the Euclidean distances between the GUs and their respective associated UAV-BSs. The minimization of this cost function holds significant importance, as shorter 2D distances correspond to higher channel gains, consequently leading to enhanced data rates for the users. As the users' locations are known, the K-means algorithm effectively clusters users based on their 2D distances from cluster centers. We use a modified K-means clustering algorithm to approximately balance user distribution across N groups while minimizing the cost function, assuming identical payload characteristics and transmit power for all UAV-BSs [55].

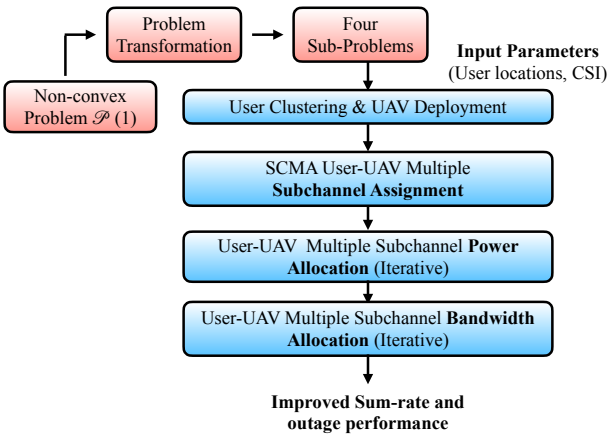

Fig. 3. Schematic representation of the proposed problem transformation and solution approach.

With given UAVs 2D location and their association, the optimization problem of the UAVs' altitudes is expressed as:

$$\mathcal{P}(\text{SP}_2): \quad \max_{h_n^{\text{uav}}} \sum_{n=1}^{N}\sum_{j=1}^{J_n} R_{n,j} \tag{12a}$$

$$\text{s.t.} \quad H_{\min} \le h_n^{\text{uav}} \le H_{\max}. \tag{12b}$$

Given the impact of LoS and NLoS components on channel gain, problem $\mathcal{P}(\text{SP}_2)$ is still nonconvex. To address this, we employ the GSS method to optimize the altitude of the nth UAV [56]. We sequentially explore the optimal altitude of each UAV to derive a suboptimal solution for subproblem $\mathcal{P}(\text{SP}_2)$. After determining the altitudes for all UAVs, the sum-rate is updated. This iterative process continues until convergence of the objective function is achieved.

B. Designing Factor graph matrix

With known $\mathbf{L}, \mathbf{C}, \mathbf{V}$, and $\mathbf{P}$, the optimization problem $\mathcal{P}(1)$ is reformulated as:

$$\mathcal{P}(\text{A2}): \quad \max_{\mathbf{F}} f_{\text{A2}}(\mathbf{F}) = \sum_{n=1}^{N}\sum_{j=1}^{J_n} \mathbf{R}_{n,j} \tag{13a}$$

$$\text{s.t.} \quad (9\text{h}), (9\text{i}), (9\text{j}), (9\text{k}). \tag{13b}$$

To solve the problem $\mathcal{P}(\text{A2})$, we introduce three heuristic algorithms to design $\mathbf{F}$.

1) CSI-based continuous Subchannel allocation (CCSA) scheme: In **Algorithm 1**, we first find out the UAV which is closest to origin. Let the location of UAV closest to origin is $\mathbf{l}_{n'}, n' \in \mathcal{N}$. Calculate the distance of all other UAVs except n' UAV, i.e., $\mathbf{l}_n, n \in \mathcal{N} \setminus \{n'\}$ from $\mathbf{l}_{n'}$. Sort the distance in ascending order and store the indices of corresponding UAVs as $\mathbf{t}$. Let a_n denotes the beginning index for subchannel allocation of the nth UAV, and $e_n = a_n + K$ designates its endpoint. For instance, with $(a_n, e_n) = (2, 2+K)$, subchannels from $k = 2$ to $k = K+2$ are assigned to the nth UAV. The start-end indicator of n'th UAV will be

Algorithm 1: The CSI-based continuous subchannel allocation (CCSA) scheme for designing **F** for multi-UAV SCMA network

Inputs:
$\mathbf{L}, \acute{d}, J_n, K_{\text{net}}, K, d_f, d_v, \mathbf{G}$.
Output:
F.

1: The subchannel end indicator is $e_{\acute{n}} = K_{\text{net}} - (\acute{n}-1)\acute{d}$. This will continue until $K \leq e_{\acute{n}} \leq K + \acute{d}$.
2: UAVs are divided into N_i number of sub-groups each having maximum n_o UAVs. Assume that the set of UAVs belonging to ith sub-group is $\mathcal{N}_i$.
3: **for** each subgroup $\mathcal{N}_i$ **do**
4: Find the UAV which is closest to origin and allocate the starting K number of suchannels to n'th UAV. Let the location of UAV closest to origin is $\mathbf{l}_{n'}, n' \in \mathcal{N}_i$.
5: Calculate distance between $\mathbf{l}_n, \{n \in \mathcal{N}_i \setminus \{n'\}\}$ and $\mathbf{l}_{n'}$.
6: Sort the distance in descending order and store the indices of corresponding UAVs as **t**.
7: The subchannels end indicator follows $e_{\acute{n}} = K_{\text{net}} - (\acute{n}-1)\acute{d}, \forall\ \acute{n} = 1 : n_o - 1 \in \mathbf{t}$. Similarly, the start indicator becomes $a_{\acute{n}} = e_{\acute{n}} - K$.
8: **for** $\breve{n} = 1 : n_o$ **do**
9: Calculate the average RMS value, **r** from **G** with respect to each user and sort them in the descending order. Save the indices of corresponding users in $\breve{J}_{\breve{n}}$.
10: **for** $\breve{i} = 1 : \breve{J}_{\breve{n}}$ **do**
11: **if** $\sum_{j=1}^{J_{\breve{n}}} \mathbf{F}_{k,j} \leq d_f,\ \forall\ a_{\breve{n}} \leq k \leq e_{\breve{n}}$ or $\mathbf{F}_{\breve{n},i} \neq \mathbf{F}_{\breve{n},j}$ **then**
12: Identify the highest d_v values from the column of **G** corresponding to index $\mathbf{r}(\breve{n}, \breve{i})$.
13: For d_v selected values in Step 12, the corresponding indices in $\mathbf{F}_{\breve{n}}$ are assigned a value of one.
14: Assign zero to the $(\breve{n}, \breve{i})$th column in **G**.
15: **else**
16: Proceed with similar Steps 12-14 for the indices corresponding to the subsequent d_v largest values.
17: **end if**
18: **end for**
19: **end for**
20: **end for**

$(a_1, e_1) = (1, K)$, i.e., $k = 1 : K$ subchannels are allocated to n'th UAV. So, the end indicator will follow an arithmetic progression as $e_{\acute{n}} = K_{\text{net}} - (\acute{n}-1)\acute{d}$, where $\acute{d}$ is the shift in the subchannel for each UAV. This will continue until $K \leq e_{\acute{n}} \leq K + \acute{d}$. Thus, out of N UAVs, subchannel allocation is done in a group of every $n_o = \frac{K_{\text{net}} - e_{\acute{n}}}{\acute{d}} + 2$ UAVs. In this manner, the start-end indication of subchannel allocation for each UAV is done.

Subsequently, the root mean square (RMS) of **G** is computed for each user and sorted in the descending order. The process of RE allocation is initiated with the user holding the maximum of the RMS values. For the chosen user, we select d_v REs with the maximum SINR and allocate these to the respective user. This process is iteratively applied for all users in a sequential manner, following the descending order of RMS values. As the assignment of REs progresses for the GUs, complying with the (9i), (9j), and (9k) constraints becomes increasingly challenging. In such instances, the algorithm sequentially selects the next d_v REs with the highest CSI values until all specified constraints are satisfied. Consequently, the proposed algorithm prioritizes assigning subchannels to users based on favorable CSI, while taking into account the SCMA FGM constraints.

2) SINR-based continuous Subchannel allocation (SCSA) scheme: In this scheme, the start-end indicator for subchannel allocation and dividing the UAVs into subgroups is done in the same manner as in CCSA scheme. In this scheme, we go one step further and allocate the subchannels to users based on SINR. For each subgroup of UAV, we begin with an initial matrix $\mathbf{F}_{\text{ini}}$, which is an all-ones matrix of size $K \times J_n$. Subsequently, we calculate the SINR matrix $\mathbf{S}_{K \times J_n} = (\gamma_{k,j})_{K \times J}$ for first UAV of this subgroup considering only intra-UAV interference, where $\gamma_{k,j}$ is as shown in (8). Following this, the RMS of **S** is computed for the users and subsequently organized in the decreasing order. The allocation of RE begins with the user holding the maximum of all the RMS values. Next, the steps similar to Steps 12-16 are followed as in Algorithm 1. The difference here is that instead of **G**, the REs are allocated based on SINR matrix **S**, considering the constraints in (9i), (9j), (9k). This procedure is further repeated for other UAVs of the subgroup, where inter-UAV interference is now considered in computing **S** from the clusters for which the FGM is already designed.

3) CSI-based Flexible Subchannel allocation (CFSA) scheme: In the above two schemes, we used start to end indicator to allocate the continuous subchannels for each UAV. In this scheme, we flexibly allocate $K < K_{\text{net}}$ subchannels to each UAV. Here, we consider inclusion of $K_{\text{net}} - K$ zero rows as a constraint in designing FGM. Next, the RMS of **G** is calculated concerning the users and subsequently arranged in the decreasing order. The allocation of RE is initiated from the user with the maximum of the RMS values. For each of the chosen user, we choose d_v REs with the maximum CSI values and allocate these REs to the respective user. This process continues until the number of non-zero rows in FGM reaches K. Once K subchannels are occupied, the rest of the highest d_v number of CSI values are chosen among only these already occupied subchannels. As the number of users increases, meeting the constraints outlined in (9i), (9j), and (9k) becomes progressively challenging. In such scenarios, the selection of the next d_v REs corresponding to the next highest CSI values continues iteratively until all specified constraints are satisfied. Thus, in the proposed scheme, the subchannels are flexibly chosen based on available CSI values.

C. Power Allocation

For the given **L**, **C**, **F**, **V**, the optimization problem $\mathcal{P}(1)$ is expressed as:

$$\mathcal{P}(\text{A3}): \quad \max_{\mathbf{P}} f_{\text{A3}}(\mathbf{P}) = \sum_{n=1}^{N} \sum_{j=1}^{J_n} \mathbf{R}_{n,j} \tag{14a}$$

$$\text{s.t.} \quad (9\text{l}), (9\text{m}). \tag{14b}$$

Algorithm 2: The Power allocation algorithm for SCMA-assisted multi-UAV network

Inputs:
$J_n, K_{\text{net}}, K, d_f, d_v, \mathbf{S}_{N\times K_{\text{net}}\times J_n}, \mathbf{F}_{N\times K_{\text{net}}\times J_n}, \mathbf{R}_{N\times K_{\text{net}}\times J_n}$.
Output: **P**.

for each subgroup $\mathcal{N}_i$ **do**
  for $n = 1 : n_o$ **do**
    Sort the rate of all the users in the descending order and store their indices.
    The user set is partitioned into two equal sub-groups: first sub-group consists of high data rate users, i.e., SG_{high} and second sub-group consists of low data rate users, i.e., SG_{low}.
    For each user, sort the SINR values on the active subchannels in ascending order.
    while $SR_n^{ii} - SR_n^{ii-1} \geq \epsilon,\ p_{n,k,j} \geq p_{\min}$ and $\text{P}_n^{ii} \leq \text{P}_{\text{tot}}$ **do**
      For the first sub-group SG_{high}, the power at small SINR channel is updated as $pi_{k,j} - pa_{k,j}$ and at large SINR channels as $pi_{k,j} + pa_{k,j}$.
      For the second sub-group SG_{low}, the power at small SINR channel is updated as $pi_{k,j} - pb_{k,j}$ and at large SINR channels as $pi_{k,j} + pb_{k,j}$.
      Update the scaling factors $pa_{k,j}^{ii} = pa_{k,j}^{ii-1} + \text{pa}_{k,j}^{ii-1}/2$ and $pb_{k,j}^{ii} = pb_{k,j}^{ii-1} + pb_{k,j}^{ii-1}/2$.
    end while
  end for
end for

Algorithm 3: The Non-uniform bandwidth allocation for multiple UAV SCMA network

Inputs: $K_{\text{net}}, \mathbf{R}_{N\times K_{\text{net}}\times J_n}$.
Output: **V**.

for each subgroup $\mathcal{N}_i$ **do**
  From **R**, sort the rate of all the users in the ascending order. Find the indices of u_a number of users with lowest data rate and save it in the set $\mathcal{U}_a$.
  For each user in the set $\mathcal{U}_a$, find the subchannels with maximum data rate and store them in the set $\mathbb{K}$. Find the unique subchannels among $\mathbb{K}$ and save them in $\mathbb{K}_s$ and remaining subchannels are stored in $\mathbb{K}_r$.
  Let K_s be number of unique subchannels and $K_r = K_{\text{net}} - K_s$ be number of remaining subchannels.
  while $R_{\text{min}}^{ii} - R_{\text{min}}^{ii-1} \geq \epsilon'$,$\text{SR}_n^{ii} - SR_n^{ii-1} \geq \epsilon,$ and $\frac{Kr_{\text{fac}}}{K_r} \geq \upsilon$ **do**
    for $k = 1 : K_s$ **do**
      $\mathbf{R}^{ii}(n, \mathbb{K}_s(k), :) = s_a\ \mathbf{R}^{ii-1}(n, \mathbb{K}_s(k), :)$
    end for
    Update $Ks_{\text{fac}} = s_a K_s$ and $Kr_{\text{fac}} = K_{\text{net}} - K_s$.
    for $k = 1 : K_r$ **do**
      $\mathbf{R}^{ii}(n, \mathbb{K}_r(k), :) = \frac{Kr_{\text{fac}}}{K_r}\ \mathbf{R}^{ii-1}(n, \mathbb{K}_r(k), :)$
    end for
    Update the scaling factor as $sa^{ii} = sa^{ii-1} + \frac{sa^{ii-1}}{2}$.
  end while
end for

Here, addressing subproblem $\mathcal{P}(\text{A3})$ presents a challenge due to its non-convexity, and the computational complexity involved in determining the optimal solution is prohibitive. To effectively address the optimization problem $\mathcal{P}(\text{A3})$, we introduce a heuristic power allocation algorithm outlined in **Algorithm 2**. This algorithm is structured to allocate power among users over the active subchannels, prioritizing those with better rate values. After solving problem $\mathcal{P}(A2)$, we get the rate for each group of users with uniform power allocation. We sort the rate of users of each group in the descending order. With computation of **F** in previous subsection, we also identify the active user-subchannel pairs. Each group of users are partitioned into two sub-groups: one with low data rate users and the other with high data rate users. Let $pi_{k,j}$ be the initial power allocated to the jth user at the kth subchannel. Since SINR is known for each user at each subchannel, we can also group the subchannels in low, moderate and high SINR subchannels for each user. Let $pa_{k,j}$ and $pb_{k,j}$ be the power scaling factors for the low and high data rate users, respectively. We initiate the power allocation by assigning the power of $pi_{k,j} - pa_{k,j}$ to low SINR subchannels and $pi_{k,j} + pa_{k,j}$ to high SINR subchannels for the low data rate user sub-group. Analogously, for the high data rate user sub-group, low SINR subchannels are allocated the power of $pi_{k,j} - pb_{k,j}$, while large SINR subchannels receive the power of $pi_{k,j} + pb_{k,j}$. Let $SR_n^{ii} = \sum_{k=1}^{K_{\text{net}}} \sum_{j=1}^{J_n} R_{n,k,j}^i$ be the sum-rate and $P_n^{ii} = \sum_{k=1}^{K} \sum_{j=1}^{J_n} f_{n,k,j} p_{n,k,j}$ be the total power of the nth cluster users at ith iteration. The values of $pa_{k,j}$ and $pb_{k,j}$ are iteratively updated until fractional increase in sumrate is above 1% and allocated power at for each user is above the minimum power p_{min} required at each subchannel.

D. Non-uniform Bandwidth allocation

For the given **L**, **C**, **F**, **P**, the optimization problem $\mathcal{P}(1)$ is reformulated as:

$$\mathcal{P}(\text{A4}): \quad \max_{\mathbf{V}} f_{\text{A4}}(\mathbf{V}) = \sum_{n=1}^{N} \sum_{j=1}^{J_n} \mathbf{R}_{n,j} \tag{15a}$$

$$\text{s.t.} \quad (9\text{n}). \tag{15b}$$

We propose **Algorithm** 3 to adjust the bandwidth of each subchannel with the aim of maximizing the sumrate and also improve the minimum user data rate. In this algorithm, for each subgroup of UAVs, we compute the data rate of all the associated users. Next, we find u_a number of users with lowest data rates and save them in the set $\mathcal{U}_a$. For these low data rate users, we find the subchannels with maximum data rate and store them in the set $\mathbb{K}$. The unique subchannels are stored in $\mathbb{K}_s$ and remaining subchannels are stored in $\mathbb{K}_r$. Next, the bandwidth associated with subchannels in $\mathbb{K}_s$ are scaled by a factor of s_a. The remaining subchannels are scaled by the factor $\frac{Kr_{\text{fac}}}{K_r}$, where $Kr_{\text{fac}} = K_{\text{net}} - K_s$. The factor s_a is updated by $sa = sa + \frac{sa}{2}$ until fractional increase in minimum rate R_{min} and sum-rate is above their defined threshold values and $\frac{Kr_{\text{fac}}}{K_r} \geq \upsilon$, where υ is the threshold ratio for the bandwidth allocation.

E. Complexity

Now, we will delve into the computational complexity of the proposed resource allocation algorithms. The

complexity of UAV deployment and user association is $\mathcal{O}(M\lceil(M/N)\rceil L_1 + L_1^{'}\log_2([h_{\max} - h_{\min}]/\epsilon))$, where L_1 denotes the number of iterations required for UAV 2D deployment and user association, $L_1^{'}$ is the number of iterations for GSS method and ϵ is the search accuracy in GSS method [56].

The computational complexity of subchannel allocation using CCSA scheme is $\mathcal{O}(N_i((n_o-1)a1+n_oJK))$, where $a1$ denotes the complexity of computing the start-end indicator for each UAV as shown in Step 7 of Algorithm 1. The computational complexity of SCSA scheme is $\mathcal{O}(N_i((n_o - 1)a1 + n_oa2JK))$, where $a2$ denotes the complexity of computing the SINR matrix for each UAV. Next, the computational complexity of CFSA scheme is $\mathcal{O}(N_i(n_oJa3K_{\text{net}}))$, where $a3$ denotes the complexity of finding the maximum d_v number of subchannels with highest CSI values, considering $K_{\text{net}} - K$ zero rows among total K_{net} rows.

The algorithmic time complexity for Algorithm 2 is $\mathcal{O}(N_in_oL_2a4)$, where L_2 is the number of iterations for power allocation and $a4$ is the complexity to compute Steps 7-9 in each iteration. The computational complexity of Algorithm 3 is $\mathcal{O}(N_iL_3(K_s + K_r))$, where L_3 represents the number of iterations for bandwidth allocation.

IV. Results and Discussion

This section presents and discusses the simulation results to demonstrate the effectiveness of the proposed resource allocation algorithms. The simulation setup comprises of five UAV-BSs serving 50 GUs distributed over 1000 m $\times$ 1000 m area. The simulation parameters are: $\alpha = 2.4$, $\eta_{\text{LoS}} = 3$ dB, $\eta_{\text{NLoS}} = 23$ dB, $a = 11.95$ and $b = 0.136$. The initial transmit power of each UAV is distributed equally among all the served users. Two benchmark schemes are considered for comparative analysis [57]:

- OMA: In this scheme, all the UAVs serve the GUs in orthogonal time slots of equal size, but they share the same frequency band. Thus, the users face only the inter-UAV interference in this case. The rate achieved by the (n, j)th user is

$$\mathbf{R}_{n,j}^{\text{OMA}} = \frac{1}{J_n}\log_2\left(1 + \frac{||g_{n,k,j}||^2 P_{\text{tot}}}{I_{n,k,j}^{\text{inter}} + \sigma^2}\right) \quad (16)$$

- Interference Free (IF): In this approach, each UAV serves GUs in orthogonal time slots and is allocated orthogonal frequency bands. Thus, the users do not face any interference and all UAVs operate with maximum transmit power. The rate achieved in IF case by the (n, j)th user is:

$$\mathbf{R}_{n,j}^{\text{IF}} = \frac{1}{NJ_n}\log_2\left(1 + \frac{||g_{n,k,j}||^2 P_{\text{tot}}}{\frac{\sigma^2}{N}}\right) \quad (17)$$

Fig. 4 shows the 3D deployment of five UAV-BSs alongside the locations of 50 GUs for SCMA, OMA and PD-NOMA schemes. Users associated with distinct UAVs are represented by varying colors, and the color of the associated UAV-BS corresponds to that of its users. Each UAV-BS is

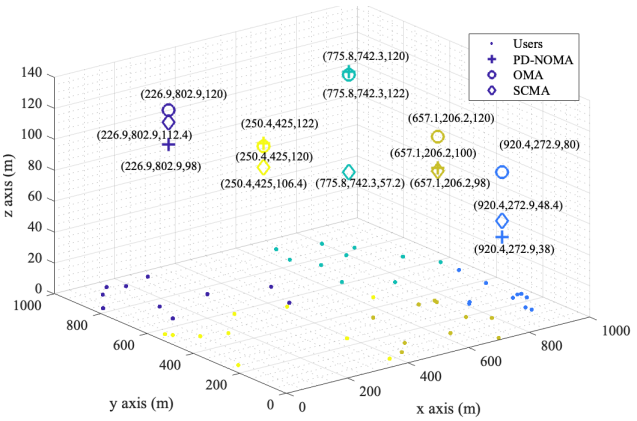

Fig. 4. 3D placement of five UAVs serving 50 users.

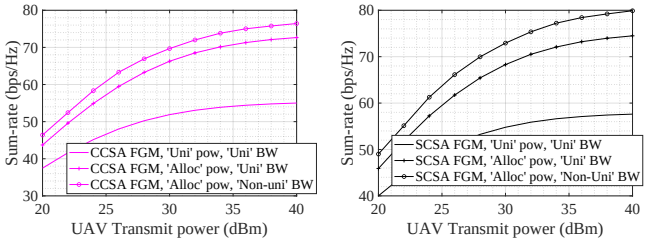

(a) CCSA scheme (b) SCSA scheme

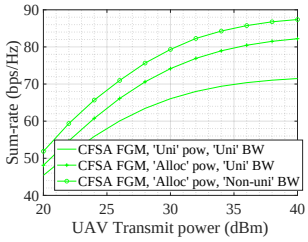

(c) CFSA scheme

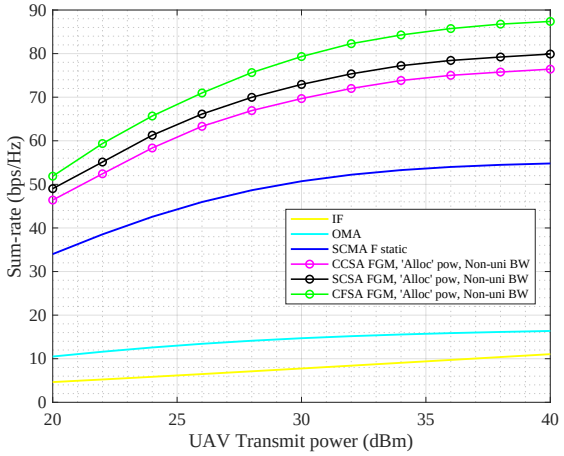

(d)

Fig. 5. Sum-rate versus UAV transmit power (a) CCSA (b) SCSA (c) CFSA based FGM, 'Uni' denotes uniform, 'Alloc' denotes allocated power from Algorithm 2 and 'Non-uni' denotes the non-uniform bandwidth allocation from Algorithm 3. Subfigure (d) shows the sum-rate performance for proposed SCMA based schemes, static FGM, OMA and IF schemes.

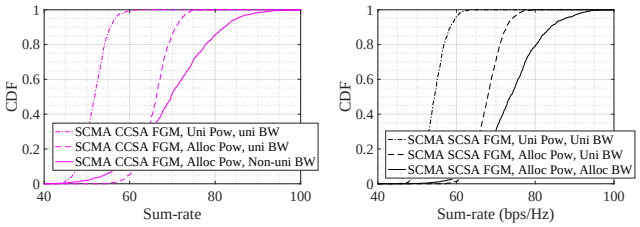

(a) CCSA scheme (b) SCSA scheme

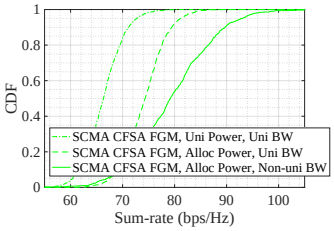

(c) CFSA scheme

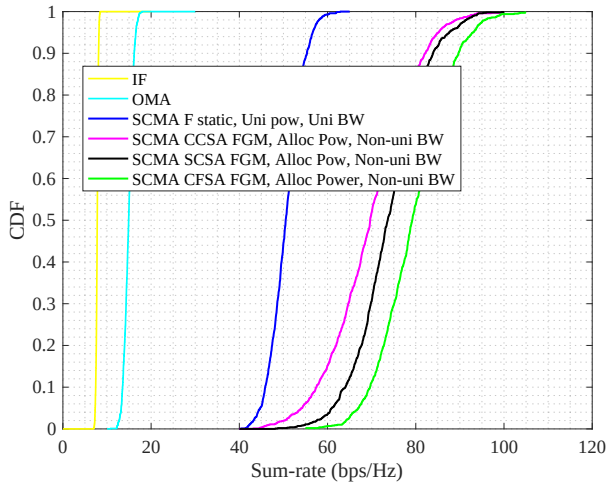

(d)

Fig. 6. CDF plot for multi-UAV SCMA network for (a) CCSA (b) SCSA (c) CFSA based FGM, 'Uni' denotes uniform, 'Alloc' denotes allocated power from Algorithm 2 and 'Non-uni' denotes the non-uniform bandwidth allocation from Algorithm 3. Subfigure (d) shows the CDF plot for proposed SCMA based schemes, static FGM, OMA and IF schemes.

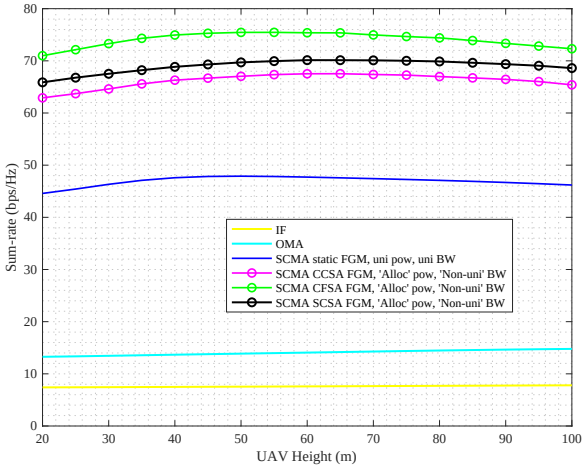

Fig. 7. Sum-rate performance as the altitude of UAVs varies, where 'Uni.' represents uniform, 'Alloc.' represents the allocated, 'Non-uni' represents non-uniform SBs allocation.

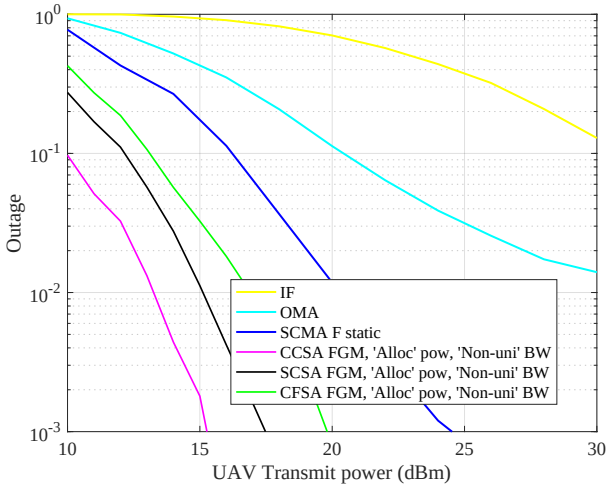

Fig. 8. Outage performance, where 'Uni.' represents uniform, 'Alloc.' represents the allocated, 'Non-uni' represents non-uniform bandwidth (BW) allocation.

positioned at the geometric center of its designated cluster in 2D space. The altitude of each UAV is fine-tuned utilizing the GSS scheme to enhance the overall sum-rate.

Fig. 5 illustrates the sum-rate performance with respect to the increase in transmit power of each UAV. In Fig. 5 (a), the **F** matrix is designed using CCSA scheme as discussed in **Algorithm 1**. Then, we have shown the impact of power allocation and non-uniform bandwidth allocation from **Algorithm 2** and **Algorithm 3**, respectively. It is noted that by introducing the proposed schemes gradually, the sum-rate of the overall network improves significantly. In Fig. 5 (b) and (c), the **F** matrix is designed using SCSA scheme and CFSA scheme, respectively. Again, for the resulting **F** matrix in both cases, we have shown the impact of power allocation and non-uniform bandwidth allocation. Fig. 5 (d) illustrates the sum-rate performance for the proposed SCMA and benchmark schemes. Here, SCMA **F** static denotes the static FGM for all clusters with uniform power and bandwidth allocation to all users. It is apparent that the sum-rate performance experiences a significant enhancement with the increase in the transmit power for all the proposed algorithms.

Fig. 6 depicts the cumulative distribution function (CDF) of the network sum-rate with respect to IF, OMA, and different SCMA schemes. In Fig. 6 (a), the **F** matrix is designed using CCSA scheme and then power allocation and bandwidth allocation is done using **Algorithm 2** and **Algorithm 3**, respectively. It is noteworthy that the gradual implementation of the proposed resource allocation schemes significantly improves the network's sum-rate. In Fig. 6 (b) and (c), the **F** matrix is designed using SCSA scheme and CFSA scheme, and in both cases, we have shown the impact of power allocation and non-uniform bandwidth allocation.

Fig. 6 (d) illustrates the CDF curves for the proposed SCMA and the benchmarking schemes. It is noteworthy that the benefits derived from the proposed methodologies exhibit stability, with the depicted curves maintaining consistent alignment with their corresponding counterparts in Fig. 5.

Fig. 7 illustrates the sum-rate performance with varying UAV altitudes for the proposed SCMA resource allocation algorithms and the benchmarking schemes. The plot reveals an initial increase followed by a subsequent decrease in the total sum-rate as the altitude increases in all the multiple access schemes, excluding IF. Therefore, optimizing the height of each UAV is a crucial factor to significantly enhance the overall network performance. Fig. 8 illustrates the outage performance of the proposed SCMA resource allocation algorithms in comparison with the benchmarking schemes. Here, the network is said to be in outage if the average minimum user rate of each cluster is less than 0.01 bps/Hz. This shows that, with the implementation of the proposed algorithms, both the sum-rate and outage performance of the network improves.

V. Conclusion

This work presents resource allocation schemes aimed to maximize the sum-rate in a SCMA-aided multiple UAV downlink system, addressing challenges related to inter-UAV and intra-UAV interferences. We have worked on the joint optimization of UAV-users association, UAV-BSs 3D deployment, multiple subchannels assignment, power allocation and bandwidth allocation to improve the network performance. We have decomposed the formulated optimization problem into four tractable subproblems and then solve them sequentially. The simulation results demonstrate that optimizing subchannel allocation, power allocation, and bandwidth allocation in a multi-UAV SCMA system can significantly enhance the achieved sum rate. The findings also indicated that 1) minimizing interference requires efficient subchannel assignment, 2) network performance benefits from balanced power allocation, and 3) optimizing bandwidth allocation helps in improving outage performance. In this work, we investigated the resource management in multi-UAV network, but UAVs face a challenge of limited energy problem. To further improve the network performance, the problem of energy consumption and channel estimation in the considered SCMA-assisted UAV networks are interesting topics for future work.

References

[1] (2021). *6G Flagship*. Accessed: Jun. 29, 2021. [Online]. Available: https://www.oulu.fi/6gflagship

[2] Cisco. (Mar. 2020). *Cisco Annual Internet Report (2018–2023) White Paper*. [Online]. Available: https://www.cisco.com/c/en/us/solutions/collateral/executive-perspectives/annual-internet-report/white-paperc11- 741490.html

[3] Y. Liu et al., "Evolution of NOMA toward next generation multiple access (NGMA) for 6G," *IEEE J. Sel. Areas Commun.*, vol. 40, no. 4, pp. 1037–1071, Apr. 2022.

[4] M. Mozaffari *et al.*, "A tutorial on UAVs for wireless networks: Applications, challenges, and open problems," *IEEE Commun. Surveys Tuts.*, vol. 21, no. 3, pp. 2334–2360, 3rd Quart., 2019.

[5] D. W. Matolak and R. Sun, "Air–ground channel characterization for unmanned aircraft systems—Part III: The suburban and near-urban environments," *IEEE Trans. Veh. Technol.*, vol. 66, no. 8, pp. 6607–6618, Aug. 2017.

[6] S. M. R. Islam *et al.*, "Power domain non-orthogonal multiple access (NOMA) in 5G systems: Potentials and challenges," *IEEE Commun. Surveys Tuts.*, vol. 19, no. 2, pp. 721–742, 2nd Quart., 2017.

[7] H. Nikopour and H. Baligh,"Sparse code multiple access," in *Proc. IEEE 24th Int. Symp. Pers. Indoor Mobile Radio Commun. (PIMRC)*, London, UK, 2013, pp. 332–336.

[8] G. Song, X. Wang, and J. Cheng, "Signature design of sparsely spread code division multiple access based on superposed constellation distance analysis," *IEEE Access*, vol. 5, pp. 23809–23821, 2017.

[9] L. Lu *et al.*, "Prototype for 5G new air interface technology SCMA and performance evaluation," *China Commun.*, vol. 12, no. 9, pp. 38–48, Sep. 2015.

[10] M. Moltafet *et al.*, "Comparison study between PD-NOMA and SCMA," *IEEE Trans.Veh. Technol.*, vol. 67, no. 2, pp. 1830–1834, Feb. 2018.

[11] Q. Luo *et al.*, "An error rate comparison of power domain non-orthogonal multiple access and sparse code multiple access," *IEEE Open J. Commun. Soc.*, vol. 2, pp. 500–511, 2021.

[12] S. Chaturvedi *et al.*, "A Tutorial on Decoding Techniques of Sparse Code Multiple Access," *IEEE Access*, vol. 10, pp. 58503-58524, 2022.

[13] H. Wen, W. Yuan, Z. Liu and S. Li, "OTFS-SCMA: A Downlink NOMA Scheme for Massive Connectivity in High Mobility Channels," *IEEE Trans. Wireless Commun*, vol. 22, no. 9, pp. 5770-5784, Sept. 2023.

[14] T. Hou, Y. Liu, Z. Song, X. Sun and Y. Chen, "Exploiting NOMA for UAV Communications in Large-Scale Cellular Networks," *IEEE Trans. Commun.*, vol. 67, no. 10, pp. 6897-6911, Oct. 2019.

[15] X. Pang *et al.*, "Uplink precoding optimization for NOMA cellular-connected UAV networks," *IEEE Trans. Commun.*, vol. 68, no. 2, pp. 1271–1283, Feb. 2020.

[16] N. Senadhira *et al.*, "Uplink NOMA for cellular-connected UAV: Impact of UAV trajectories and altitude," *IEEE Trans. Commun.*, vol. 68, no. 8, pp. 5242-5258, Aug. 2020, doi: 10.1109/T-COMM.2020.2995373.

[17] S. Barick and C. Singhal, "Multi-UAV assisted IoT NOMA uplink communication system for disaster scenario," *IEEE Access*, vol. 10, pp. 34058-34068, 2022.

[18] Z. H. E. Tan *et al.*, "NOMA-aided multi-UAV communications in full-duplex heterogeneous networks," *IEEE Syst. J.*, vol. 15, no. 2, pp. 2755–2766, Jun. 2021.

[19] V.-H. Dang *et al.*, "Throughput optimization for NOMA energy harvesting cognitive radio with multi-UAV-assisted relaying under security constraints," *IEEE Trans. Cognit. Commun. Netw.*, vol. 9, no. 1, pp. 82–98, Feb. 2023.

[20] N. Zhao et al., "Security Enhancement for NOMA-UAV Networks," *IEEE Trans. Veh. Technol.*, vol. 69, no. 4, pp. 3994-4005, April 2020.

[21] D. Diao *et al.*, "Secure Wireless-Powered NOMA Communications in Multi-UAV Systems," *IEEE Trans. Green Commun. Netw.*, vol. 7, no. 3, pp. 1205-1216, Sept. 2023.

[22] M. Katwe *et al.*, "Dynamic user clustering and optimal power allocation in UAV-assisted full-duplex hybrid NOMA system," *IEEE Trans. Wireless Commun.*, vol. 21, no. 4, pp. 2573–2590, Sep. 2021.

[23] M. T. Nguyen and L. B. Le, "Multi-UAV trajectory control, resource allocation, and NOMA user pairing for uplink energy minimization," *IEEE Internet Things J.*, vol. 9, no. 23, pp. 23728–23740, Dec. 2022.

[24] R. Tang *et al.*, "Utility Maximization for Multi-UAV-Assisted IoT Sensor Systems With NOMA," *IEEE Sen. J.*, vol. 24, no. 17, pp. 28233-28250, 1 Sept.1, 2024.

[25] X. Liu, Z. Liu, and M. Zhou, "Fair energy-efficient resource optimization for green multi-NOMA-UAV assisted Internet of Things," *IEEE Trans. Green Commun. Netw.*, vol. 7, no. 2, pp. 904–915, Jun. 2023.

[26] R. Chen *et al.*, "Multi-UAV coverage scheme for average capacity maximization," *IEEE Commun. Lett.*, vol. 24, no. 3, pp. 653–657, Mar. 2020.

[27] R. Duan *et al.*, "Resource allocation for multi-UAV aided IoT NOMA uplink transmission systems," *IEEE Internet Things J.*, vol. 6, no. 4, pp. 7025–7037, Aug. 2019.

[28] A. Gupta, A Trivedi and B. Prasad, "B-GWO based multi-UAV deployment and power allocation in NOMA assisted wireless networks," *Wireless Netw*, no. 28, pp. 3199–3211, Jul. 2022.

[29] Le-Mai-Duyen Nguyen *et al.*, "Throughput analysis and optimization for NOMA Multi-UAV assisted disaster communication using CMA-ES," *Wirel. Netw.* 2021, 27, 4889–4902.

[30] J. Chen *et al.*, "Deployment for NOMA-UAV Base Stations Based on Hybrid Sparrow Search Algorithm," *IEEE Trans. Aerosp. Electron. Syst.*, doi: 10.1109/TAES.2023.3272530.

[31] S. Najmeddin *et al.*, "Energy-efficient resource allocation in multi-UAV networks with NOMA," *IEEE Trans. Green Commun. Netw.*, vol. 5, no. 4, pp. 1906–1917, Dec. 2021.

[32] N. Nouri *et al.*, "Three-dimensional multi-UAV placement and resource allocation for energy-efficient IoT communication," *IEEE Internet Things J.*, vol. 9, no. 3, pp. 2134-2152, Feb. 2022.

[33] X. Zhang *et al.*, "Energy-efficient multi-UAV-enabled multiaccess edge computing incorporating NOMA," *IEEE Internet Things J.*, vol. 7, no. 6, pp. 5613–5627, Jun. 2020.

[34] L. Lin *et al.*, "Prioritized delay optimization for NOMA-based multi-UAV emergency networks," *IEEE Trans. Veh. Technol.*, pp. 1–6, 2022.

[35] W. Mei and R. Zhang, "Uplink cooperative NOMA for cellular connected UAV," *IEEE J. Sel. Topics Signal Process.*, vol. 13, no. 3, pp. 644–656, Jun. 2019.

[36] S. Miao, N. Ye, J. Li, Y. Wang and J. Pan, "Optimal Load Allocation of On-Board Detection for Multi-UAV Cooperative NOMA under Payload Constraints," *IEEE Trans. Veh. Technol.*, doi: 10.1109/TVT.2025.3561204.

[37] J. Li, S. Dang, X. Chen, M. Wen, M. Di Renzo and H. Arslan, "Cooperative Non-Orthogonal Multiple Access With Index Modulation for Air-Ground Multi-UAV Networks," *IEEE J. Sel. Areas Commun.*, vol. 43, no. 1, pp. 171-185, Jan. 2025.

[38] P. Qin, Y. Fu, J. Zhang, S. Geng, J. Liu and X. Zhao, "DRL-Based Resource Allocation and Trajectory Planning for NOMA-Enabled Multi-UAV Collaborative Caching 6G Network," *IEEE Trans. Veh. Technol.*, vol. 73, no. 6, pp. 8750-8764, June 2024.

[39] Y. Bai, H. Zhao, X. Zhang, Z. Chang, R. Jäntti and K. Yang, "Toward Autonomous Multi-UAV Wireless Network: A Survey of Reinforcement Learning-Based Approaches," *IEEE Commun. Surveys Tuts.*, vol. 25, no. 4, pp. 3038-3067, Fourthquarter 2023.

[40] N. Deng *et al.*, "Enhancing millimeter wave cellular networks via UAV-borne aerial IRS swarms," *IEEE Trans. Commun.*, vol. 72, no. 1, pp. 524–538, Jan. 2024.

[41] Z. Lin *et al.*, "Supporting IoT With Rate-Splitting Multiple Access in Satellite and Aerial-Integrated Networks," *IEEE Internet Things J.*, vol. 8, no. 14, pp. 11123-11134, 15 July15, 2021.

[42] Z. Lin *et al.*, "Secrecy-Energy Efficient Hybrid Beamforming for Satellite-Terrestrial Integrated Networks," *IEEE Trans. Commun.*, vol. 69, no. 9, pp. 6345-6360, Sept. 2021.

[43] Z. Lin *et al.*, "SLNR-Based Secure Energy Efficient Beamforming in Multibeam Satellite Systems," *IEEE Trans. Aerosp. Electron. Syst.*, vol. 59, no. 2, pp. 2085-2088, April 2023.

[44] T. Wang, "Multi-Objective Resource Allocation for UAV-Assisted Air-Ground Integrated MC-NOMA Networks," *IEEE Access*, vol. 12, pp. 141000-141012, 2024.

[45] S. Chaturvedi *et al.*,"Trajectory Design for Sum-Rate Enhancement in UAV-SCMA System," *2023 IEEE 97th Vehicular Technology Conference (VTC2023-Spring)*, Florence, Italy, 2023, pp. 1-6.

[46] S. Chaturvedi *et al.*, "Resource Management for Sum-rate Maximization in SCMA-Assisted UAV System", *Veh. Commun.*, Dec. 2023.

[47] S. Chaturvedi *et al.*, "Resource Allocation for Sum-Rate Maximization in Multi-UAV SCMA Networks," *2023 IEEE Globecom Workshops (GC Wkshps)*, Kuala Lumpur, Malaysia, 2023, pp. 1219-1224.

[48] P. Liu, J. Lei and W. Liu, "Learning-Based Latency and Energy Optimization in SCMA-Enhanced UAV-MEC Networks," *2023 IEEE/CIC International Conference on Communications in China (ICCC)*, Dalian, China, 2023, pp. 1-6, doi: 10.1109/ICCC57788.2023.10233490.

[49] Z. Ding *et al.*, "A Survey on Non-Orthogonal Multiple Access for 5G Networks: Research Challenges and Future Trends," *IEEE J. on Selected Areas in Commun.*, vol. 35, no. 10, pp. 2181-2195, Oct. 2017.

[50] A. Al-Hourani, S. Kandeepan, and S. Lardner, "Optimal LAP altitude for maximum coverage," *IEEE Wireless Commun. Lett.*, vol. 3, no. 6, pp. 569–572, 2014.

[51] K. Zhu, X. Xu, and S. Han, "Energy-efficient UAV trajectory planning for data collection and computation in mMTC networks," in *Proc. IEEE Globecom Workshops (GC Wkshps)*, Dec. 2018, pp. 1–6.

[52] J. Lyu, Y. Zeng, and R. Zhang, "UAV-aided offloading for cellular hotspot," *IEEE Trans. Wireless Commun.*, vol. 17, no. 6, pp. 3988–4001, Jun. 2018.

[53] Z. Liu and L.-L. Yang, "Sparse or dense: A comparative study of code-domain NOMA systems," *IEEE Trans. Wireless Commun.*, vol. 20, no. 8, pp. 4769–4780, Aug. 2021.

[54] S. Boyd and L. Vandenberghe, *Convex Optimization*. Cambridge, U.K.: Cambridge Univ. Press, 2004.

[55] Y. Liu, K. Liu, J. Han, L. Zhu, Z. Xiao, and X.-G. Xia, "Resource allocation and 3-D placement for UAV-enabled energy-efficient iot communications," *IEEE Internet of Things Journal*, vol. 8, no. 3, pp. 1322–1333, 2021.

[56] Y. Chang, "N-dimension golden section search: Its variants and limitations," in *Proc. 2nd Int. Conf. Biomed. Eng. Informat.*, Oct. 2009, pp. 1–6.

[57] X. Mu, Y. Liu, L. Guo, J. Lin and H. V. Poor, "Intelligent Reflecting Surface Enhanced Multi-UAV NOMA Networks," *IEEE J. Sel. Areas Commun.*, vol. 39, no. 10, pp. 3051-3066, Oct. 2021, doi: 10.1109/JSAC.2021.3088679.